Phosphorylation Driven Motions in the COOH-terminal Src Kinase, Csk, Revealed Through Enhanced Hydrogen–Deuterium Exchange and Mass Spectrometry (DXMS)

ARTICLE *in* JOURNAL OF MOLECULAR BIOLOGY · DECEMBER 2002

Impact Factor: 4.33 · DOI: 10.1016/S0022-2836(02)01003-3 · Source: PubMed

8 AUTHORS, INCLUDING:

Patricia Jennings
University of California, San Diego
153 PUBLICATIONS **4,952** CITATIONS
SEE PROFILE

Joseph A Adams
University of California, San Diego
90 PUBLICATIONS **4,889** CITATIONS
SEE PROFILE

doi:10.1016/S0022-2836(02)01003-3 available online at http://www.idealibrary.com on IDEAL® J. Mol. Biol. (2002) 323, 871–881

JMB

Phosphorylation Driven Motions in the COOH-terminal Src Kinase, Csk, Revealed Through Enhanced Hydrogen–Deuterium Exchange and Mass Spectrometry (DXMS)

Yoshitomo Hamuro[1]†, Lilly Wong[2]†, Jennifer Shaffer[3], Jack S. Kim[1] David D. Stranz[4], Patricia A. Jennings[2], Virgil L. Woods Jr[1]* and Joseph A. Adams[3]*

[1]*Department of Medicine University of California, San Diego, 9500 Gilman Drive, La Jolla, CA 92093-0656, USA*

[2]*Department of Chemistry and Biochemistry, University of California, San Diego, La Jolla CA 92093-0656, USA*

[3]*Department of Pharmacology University of California, San Diego, La Jolla, CA 92093-0656 USA*

[4]*Sierra Analytics, LLC, 2105 Lancey Drive, Suite 1A Modesto, CA 95355, USA*

**Corresponding authors*

Previous kinetic studies demonstrated that nucleotide-derived conformational changes regulate function in the COOH-terminal Src kinase. We have employed enhanced methods of hydrogen–deuterium exchange-mass spectrometry (DXMS) to probe conformational changes on Csk in the absence and presence of nucleotides and thereby provide a structural framework for understanding phosphorylation-driven conformational changes. High quality peptic fragments covering approximately 63% of the entire Csk polypeptide were isolated using DXMS. Time-dependent deuterium incorporation into these probes was monitored to identify short peptide segments that exchange differentially with solvent. Regions expected to lie in loops exchange rapidly, whereas other regions expected to lie in stable secondary structure exchange slowly with solvent implying that Csk adopts a modular structure. The ATP analog, AMPPNP, protects probes in the active site and distal regions in the large and small lobes of the kinase domain, the SH2 domain, and the linker connecting the SH2 and kinase domains. The product ADP protects similar regions of the protein but the extent of protection varies markedly in several crucial areas. These areas correspond to the activation loop and helix G in the kinase domain and several inter-domain regions. These results imply that delivery of the γ phosphate group of ATP induces unique local and long-range conformational changes in Csk that may influence regulatory motions in the catalytic pathway.

Keywords: Csk; deuterium exchange; mass spectrometry; Src; kinase

Introduction

The Src family of non-receptor protein tyrosine kinases (nrPTKs) bind to receptor protein tyrosine kinases (rPTKs) where they phosphorylate downstream protein targets associated with discrete signaling pathways.[1–3] While the Src enzymes comprise a large subfamily of nrPTKs, all are regulated through a single nrPTK, COOH-terminal Src kinase (Csk). Csk down-regulates kinase activity by phosphorylating a single tyrosine residue in the C terminus of the Src enzymes.[4,5] Owing to this premier regulatory function, Csk has direct effects on many biological functions including T-cell activation, neuronal development, cytoskeletal organization, and cell-cycle control.[6–9] The general significance of Csk is also evident in the lethality of gene knockouts in mice.[10] Csk contains three structural components essential for *in vivo* function: a tyrosine kinase domain, an SH2 domain, and an SH3 domain. The structure of the kinase

† These authors contributed equally.

Present address: Y. Hamuro, ExSAR Corporation, Inc., 11 Deer Park Drive, Suite 103, Monmouth Junction, NJ 08852, USA.

Abbreviations used: DXMS, hydrogen–deuterium exchange mass spectrometry; ESI, electrospray ionisation; rPTK, receptor protein tyrosine kinase; nrPTK, non-receptor protein tyrosine kinase; Csk, COOH-terminal Src kinase.

E-mail address of the corresponding authors: vwoods@ucsd.edu; joeadams@ucsd.edu

domain, solved by X-ray diffraction, adopts a standard kinase fold with typical nucleotide and substrate binding lobes.[11] Unlike Src family nrPTKs, Csk is not upregulated through activation loop phosphorylation. The X-ray structures for c-Src illustrate that the C terminus is phosphorylated and interacts tightly with the SH2 domain.[12–14] In Csk, no such interaction is possible owing to the absence of a phosphorylatable sequence in the C terminus. As revealed by X-ray diffraction studies, this generates a unique domain organization where the SH2 domain interacts with the small lobe of the kinase core in Csk rather than the large lobe as in c-Src.[15]

Understanding the conformational nature of protein kinases in solution is important for evaluating function, since it has been shown that slow structural movements can limit substrate phosphorylation. The first pre-steady-state kinetic studies applied to a protein kinase, cAMP-dependent protein kinase (PKA), revealed that slow conformational changes associated with nucleotide binding and release limit catalytic cycling.[16–18] Since these early investigations, two other protein kinases have been studied using fast mixing kinetic techniques. While the tyrosine kinases Her-2 and Csk rapidly phosphorylate substrates in the active site, rate-limiting events in the catalytic cycle are associated with slow conformational changes linked to ADP release.[19,20] Although more kinetic investigations are clearly needed for a broad assessment of function, the detailed investigations into these three protein kinases reveal a common motif for activity regulation. Once ATP and the substrate are appropriately oriented in the active site, phosphoryl transfer occurs with little impediment. In contrast, the regeneration of this active complex occurs partly through slow conformational changes that appear to be linked to ADP release.

Amide hydrogen exchange techniques have proven to be increasingly powerful tools by which protein dynamics, structure and function can be probed.[21–25] Deuterium exchange methodologies coupled with either MALDI or electrospray ionisation (ESI) mass spectrometry, presently provide one of the most effective approaches to study proteins larger than 30 kDa in size. Proteolytic and/or collision-induced dissociation fragmentation methods allow exchange behavior to be mapped to subregions of the protein. In a previous study using such techniques, it was demonstrated that ADP binding induces long-range structural changes in the catalytic subunit of PKA.[26] Two of these regions encompass critical loops in the active site, as expected, whereas two other regions are distally located. These regions encompass the C terminus and helix αC. On the basis of crystallographic evidence, the latter secondary structural element is known to move in phosphorylation and subunit-dependent manner in several other protein kinases.[27,28] The exciting inference derived from these solution studies is that long-range perturbations may be coupled to slow conformational changes detected in the kinetic mechanism for PKA.[17,18] Thus, a tangible link between catalytic function and solution structure may now be established.

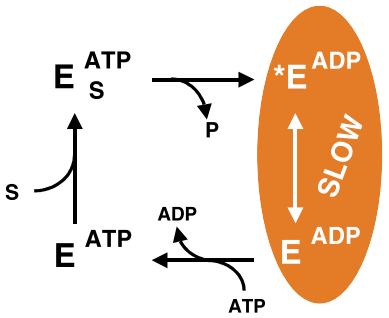

Figure 1. Catalytic pathway for Csk determined using rapid quench-flow mixing. All steps are fast relative to the slow, rate-limiting step enclosed in the oval. S, $K_4E_2IYF_4$; P, $K_4E_2IpYF_4$. These data are taken from Shaffer *et al.*[19]

Prior kinetic studies have shown that conformational changes associated with ADP release provide a regulatory mode for substrate phosphorylation in the nrPTK, Csk (Figure 1). Here, we sought to address these structural issues by monitoring the effects of nucleotide binding on the solution conformation of Csk with enhanced amide hydrogen exchange methods that we have recently developed. Despite the promise of amide exchange techniques, they have remained labor intensive and time-consuming, with substantial limitations in throughput, comprehensiveness (the extent to which a protein sequence is covered with measurable peptide fragments) and resolution (the degree to which exchange measurements can be ascribed to particular amides). Building upon the pioneering work of Englander, Smith, and co-workers[24,25,29–31] we have developed and implemented a number of improvements to these methodologies, which we collectively term hydrogen–deuterium exchange mass spectrometry (DXMS).[32–35] The studies of Csk contained here employ many of these improved methodologies.

Earlier amide hydrogen exchange techniques have been successfully applied to two protein kinases, to date; PKA[26] and ERK2.[36–38] Both kinases are structurally simple, being composed primarily of kinase domains. In comparison, Csk has more elaborate domain structure with the tyrosine kinase domain flanked by two non-catalytic SH2 and SH3 domains. These domains are thought to limit movements in the kinase core, impair nucleotide access and release and diminish catalytic activity in the structurally related c-Src.[12] Here, we have employed DXMS to demonstrate that nucleotide binding induces long-range changes in the structure of Csk. A comparison of the ATP (AMPPNP) and ADP forms reveals unique structural changes induced by the γ phosphate group of the nucleotide.

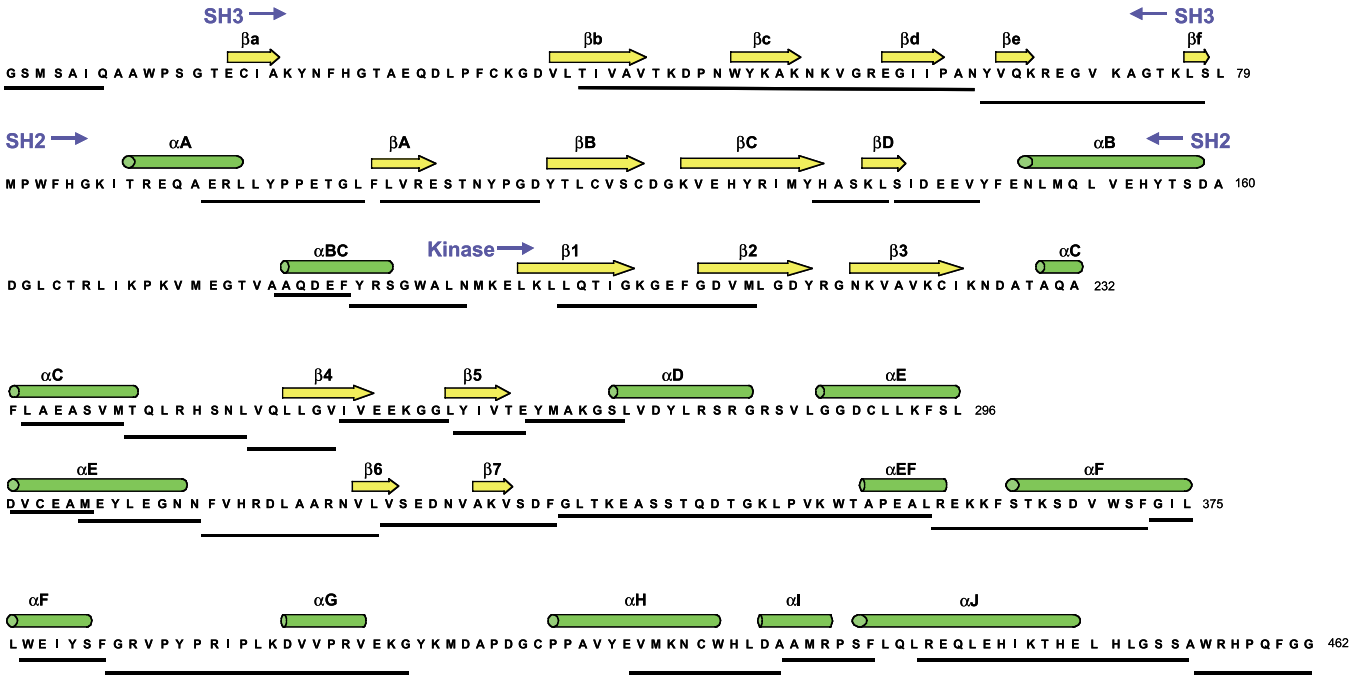

Figure 2. Peptide probes employed here mapped to the primary sequence of Csk. The designated secondary structure, domains, and loop regions are based on the three-dimensional structure of Csk.[15]

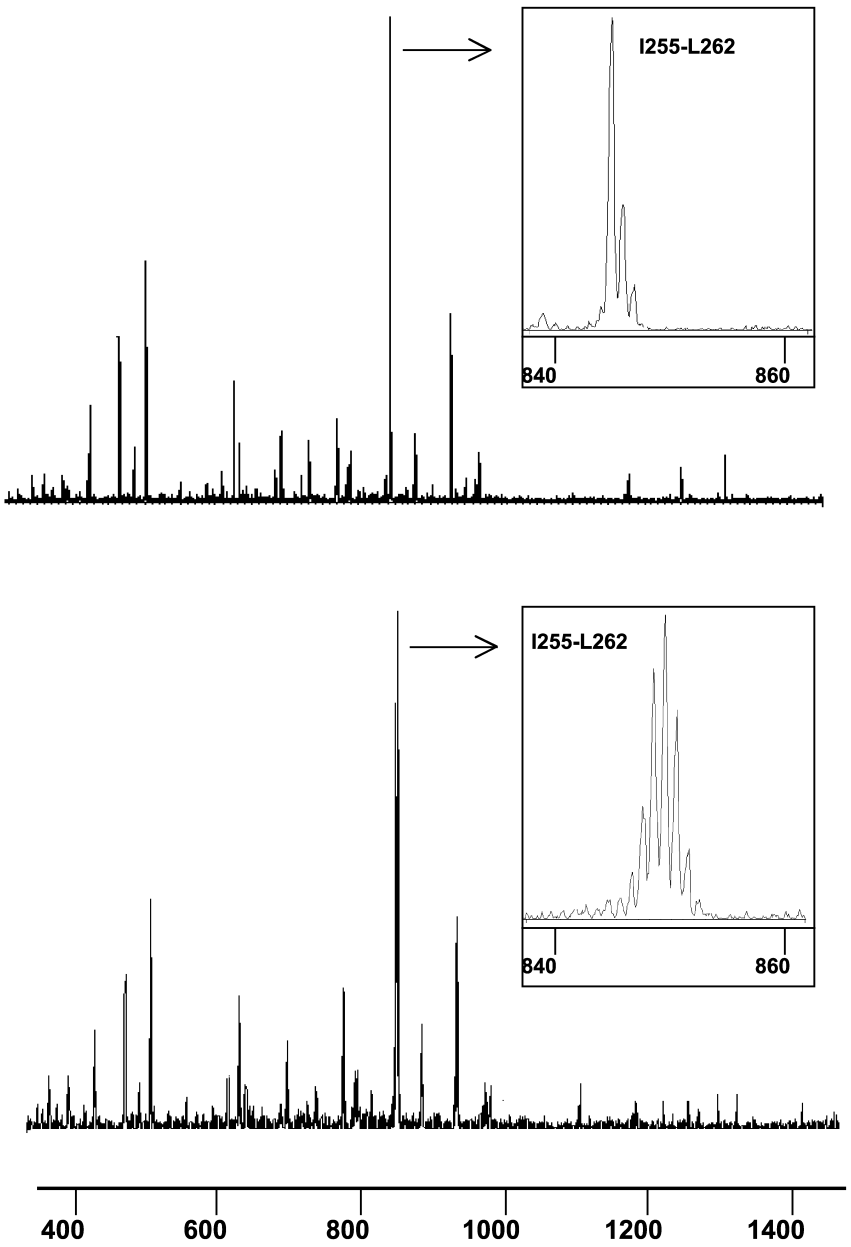

Figure 3. ESI-MS of pepsin-treated Csk before (upper panel) and after (lower panel) incubation with $^{2}H_2O$. The peak clusters corresponding to the peptide fragment, I255-L262, are shown expanded in the insets in the upper and lower panels.

These structural effects ramify not only throughout the small and large lobes of the kinase domain but also modify intra-domain dynamics.

Results

Tuning of Csk proteolytic fragmentation

Prior to studying the hydrogen exchanged samples, digestion conditions that produced Csk fragments of optimal size and distribution for exchange analysis were established (see Materials and Methods). Minimal back exchange and optimal pepsin digestion for Csk were obtained by diluting one part of the deuterated sample with one and a half parts of quench solution (0.8 M GuHCl in 0.8% formic acid). The quenched sample was then run over immobilized pepsin (66 μl bed volume) at a flow rate of 100 μl/minute, resulting in a digestion duration of 40 seconds. These conditions generated 28 high-quality peptides covering 63% of the Csk sequence (Figure 2). Since both the amino group of the first amino acid and the amide hydrogen of the second amino acid exchange too rapidly to retain deuterons during the experiment, the total number of amide hydrogen atoms followed by DXMS was 223 out of 444 non-proline residues (50%). The complete set of probes used are shown mapped (yellow) to the tertiary structure of Csk in Figure 5(a).

Deuterium incorporation into the proteolytic fragment probes

The incorporation of deuterium from solvent $^{2}H_2O$ can be monitored using DXMS. Figure 3

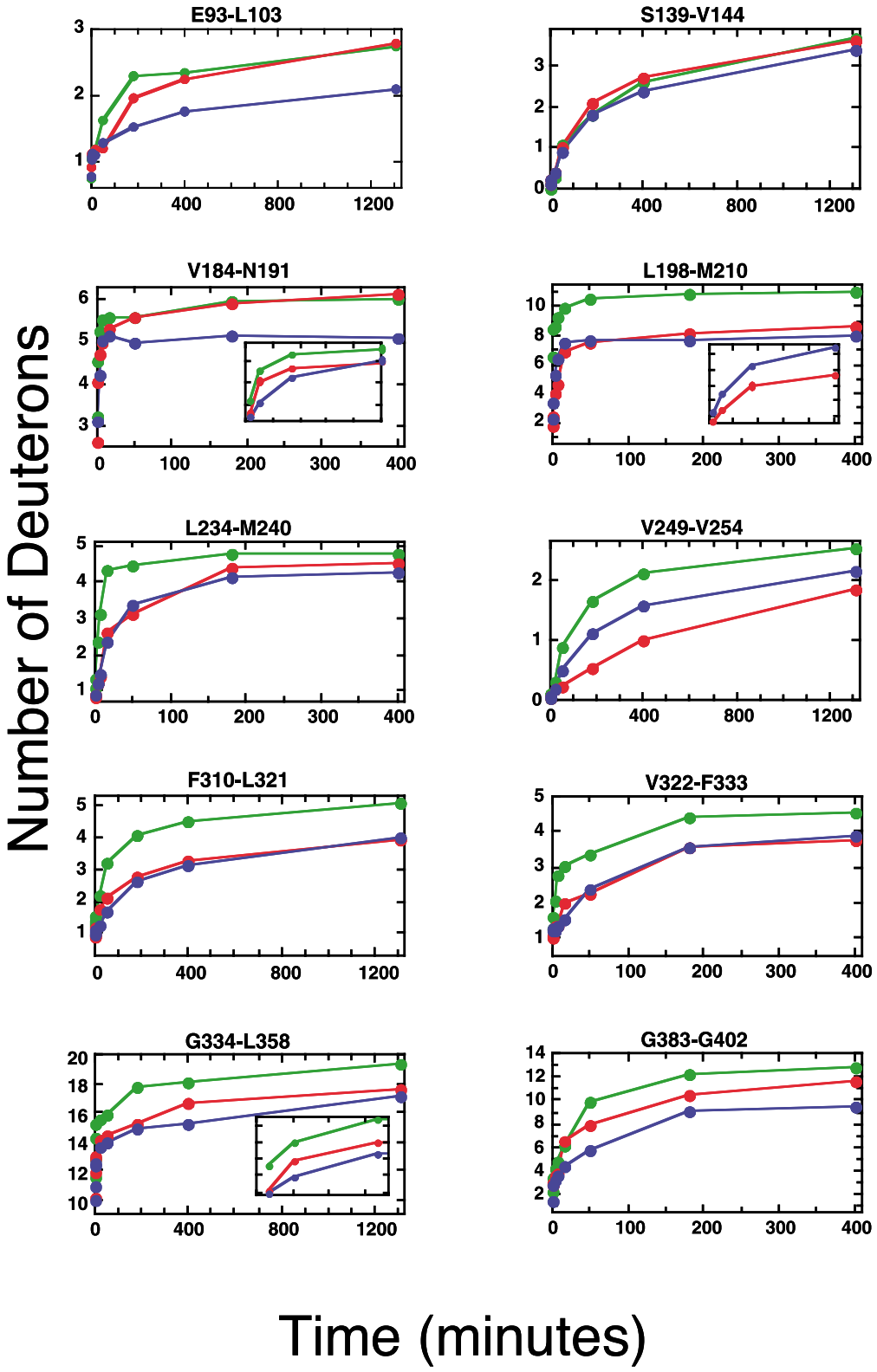

Figure 4. Time-dependent deuterium incorporation in several peptide probes in the absence and presence of nucleotides. Data shown in green, blue and red represent deuterium incorporation into apo, AMPPNP-bound, and ADP-bound forms of Csk, respectively. The probes listed in the individual plots correspond to the following structural elements based on the X-ray coordinates of Csk:[15] E93-L103 (αA in SH2), S139-V144, V184-N191 (SH2-kinase linker), L198-M210 (glycine-rich loop), L234-M240 (αC), V249-V254, F310-L321 (catalytic loop), V322-F333, G334-L358 (activation loop), and G383-G402 (αG).

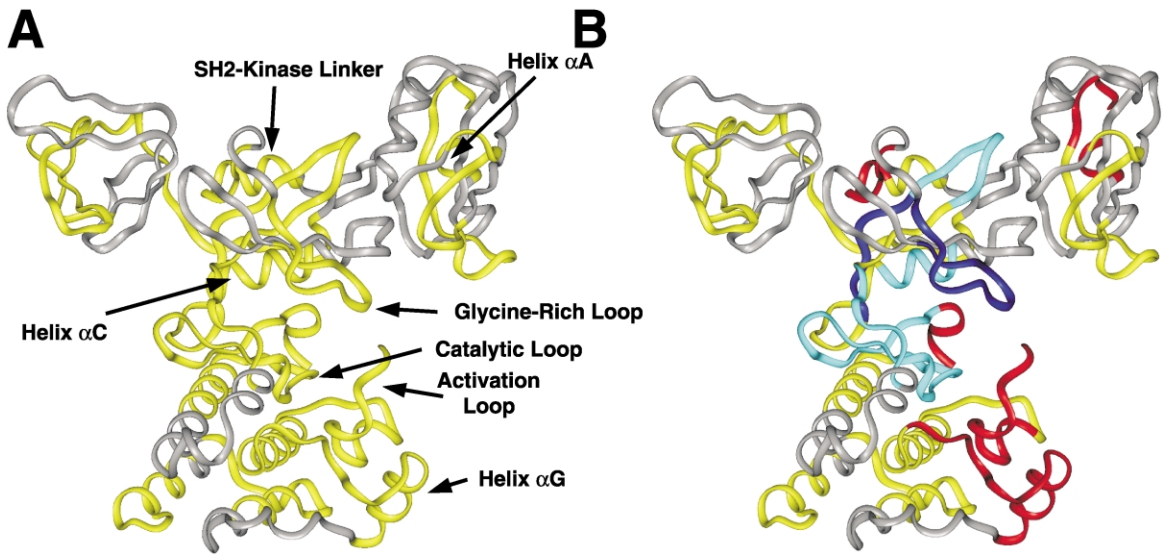

Figure 5. Effects of nucleotide binding on Csk. (a) All probes used for H–^{2}H exchange studies are mapped to the X-ray structure for Csk in yellow. Several key structural features are labeled. (b) Probes protected by AMPPNP and ADP. Probes in dark blue show greater protection in the presence of ADP than AMPPNP. Probes in red show greater protection in the presence of AMPPNP compared to ADP. Probes in yellow are not protected by either nucleotide. Probes shown in light blue are equally protected from deuterium incorporation by AMPPNP and ADP.

shows the ESI spectra of proteolyzed Csk before and subsequent to dilution into ^2H_2O. The insets in this Figure highlight one specific peptide fragment, I255-L262. This probe appears as a cluster of peaks owing to the natural isotopic distribution of the atoms in the peptide. After three hours of incubation in ^2H_2O, the envelope of peaks for the probes increases in overall mass and complexity. The centroids for these two clusters are used to determine the mass of the probe both before and after incubation with solvent deuterium.

Effects of nucleotide binding on deuterium in-exchange

The average mass of each peptide was elucidated by integrating over the full envelope of peaks. To quantify the extent of deuterium incorporation at various time periods, the mass of each probe was converted to a number of in-exchanged deuterons using equation (1). The in and back-exchange controls set the zero and infinite time points for $D(t)$. Each peptide fragment is unique with different numbers of exchangeable protons and different intrinsic exchange rates. This method detects total mass changes for each probe without defining the priority of amide exchange within each probe. Deuterium incorporation into the Csk probes was followed as a function of time in the absence and presence of two nucleotides: AMPPNP and ADP. Figure 4 displays the time-dependent incorporation of deuterium into several typical probes. In some cases (e.g. S139-V144), the presence of either nucleotide has no effect on the incorporation of deuterium over the experimental time frame (ten seconds to 1200 minutes). These probes are considered non-protected by the ligand over the exchange times studied. By comparison, the rate of deuterium incorporation into other probes is impaired by the ligand. These probes are considered protected by the nucleotide. In no case have we found that the nucleotide increases the rate of deuterium incorporation compared to the apo-enzyme. The definition of whether a probe is protected by the nucleotide over the experimental time frame depends on the accuracy of the mass measurement in the ESI spectrometer. For the set of probes used in these studies, kinetic traces that differ by more than 0.5 deuteron in mass at a minimum of two points are defined as experimentally different. Using these criteria, we have identified a number of probes whose deuteration rate is impaired by the presence of the nucleotide (Figure 4). Figure 5(b) shows the probes that are protected from exchange by AMPPNP. Furthermore, we have identified probes that are differentially protected by AMPPNP and ADP. These probes are displayed onto the Csk structure in Figure 5(b).

Discussion

Since the crystallographic solution of the first protein kinase structure approximately one decade ago,[39,40] it has become apparent that this enzyme family undergoes structural changes that are linked to activity regulation. For example, many protein kinases have been crystallized in both "open" and "closed" forms that differ by domain rotations.[41] Other protein kinases that are regulated through phosphorylation and protein binding display large movements in loop and helical regions upon activation. The cyclin-dependent protein

kinase, cdk2, and the insulin receptor kinase undergo large changes in helix αC and the activation loop when a cyclin binds in the former case and upon phosphorylation in the latter case.[27,28,42] It has also been demonstrated that discrete structural changes partially or fully limit substrate processing in several protein kinases based on pre-steady-state kinetic measurements.[17–20] Here, we have employed H–^{2}H exchange coupled with mass spectrometric methods to probe the solution conformation of the non-receptor PTK, Csk. Previous kinetic studies have shown that slow conformational changes limit ADP release (Figure 1). To address whether Csk adopts any unique structural states that may be important for regulation, the solution conformation of the full-length enzyme was studied in the absence and presence of the product, ADP, and a non-hydrolyzable ATP analog, AMPPNP.

Effects in the kinase domain

While two regions in the active site of Csk that are expected to interact with ATP (catalytic and glycine-rich loops; Figure 5) are highly protected from deuterium incorporation in the presence of AMPPNP, several regions outside the active site are also protected by nucleotide. For example, the probe encompassing helix αC (L234-M240, Figure 4) is protected by AMPPNP by as much as two deuterons over intermediate exchange time frames. Such protection has also been observed in PKA upon ADP binding.[26] This helix does not make any direct contacts with the nucleotide but rather contains a conserved residue (Glu236, Glu91 in PKA) that forms a salt bridge with another conserved residue (Lys222, Lys72 in PKA). Lys72 in PKA has been shown to form interactions with the αβ phosphate groups of ATP, suggesting that Lys222 could serve a similar function in Csk. The electrostatic dyad between these two residues (Glu-Lys) is conserved in the enzyme family and also appears to be disrupted in several down-regulated protein kinases. For example, this disruption in the InRK and cdk2 is coordinately linked to movements in helix αC.[27,28] While these motions occur upon cyclic binding for cdk2 and upon activation loop phosphorylation for the InRK, the protection observed in our H–^{2}H exchange experiments suggests that movements in this helix may be induced solely by nucleotide binding.

The association of nucleotide with Csk has profound effects on regions in the large lobe of the kinase domain. Protection of a probe containing the activation loop (G334-L358, Figures 4 and 5) suggests that this region is affected by nucleotide binding. While this loop is not expected to contact ATP directly, a conserved aspartate residue (Asp184 in PKA, Asp332 in Csk) preceding the activation loop chelates the essential, activating Mg^{2+}, which stabilizes the γ phosphate group of ATP. It is conceivable that protection in the activation loop upon AMPPNP binding in Csk may reflect conformational changes linked to movements in this preceding structural element. The binding of nucleotide to Csk has further effects on the large lobe of the kinase domain. Most notably, the probe containing helix αG is protected from deuterium incorporation by AMPPNP (Figure 5). This helix makes no direct contact with the nucleotide and is even further removed from the active site than helix αC and the activation loop. While it is not clear how AMPPNP can transmit such long-range effects across the kinase domain, space-filling models illustrate that the activation loop packs on top of helix G.[27] Such findings suggest that the binding of the nucleotide has pervasive effects on the kinase domain which ramify from their origins in the small ATP-binding lobe down to the larger substrate-binding lobe.

Inter-domain cross-talk

Prior kinetic studies have shown that the SH2 and SH3 domains of Csk enhance catalytic activity by approximately two orders of magnitude.[43,44] Such findings suggest that these domains play an important role in organizing the catalytic residues in the active site. Indeed, two regions near the interface between the SH2 and kinase domains display protection in the presence of AMPPNP (Figure 5(b)). Probes corresponding to helix αA in the SH2 domain (E93-L103, Figure 4) and a portion of the SH2-kinase linker region (Y184-N191, Figure 4) are protected by AMPPNP. In Csk, a short helix within the linker makes contacts with the kinase domain through helix αC. The coordinate protection in both the SH2-kinase linker and helix αC suggests that a "communication pathway" between the SH2 domain and active site is critical for catalytic function. Owing to protection by nucleotides of helix αA, this pathway may involve changes in the SH2 domain in addition to rigid domain–domain movements.

Phosphorylation-driven motions

The data presented thus far indicate that AMPPNP and presumably ATP induce both local and long-range movements in the kinase and neighboring SH2 domain (Figure 5(b)). It has been shown that structural changes in Csk limit the rate of release of ADP, a phenomenon that regulates function (Figure 1). To probe whether the ADP-bound complex populates a unique conformation compared to the ATP-bound form, we studied deuterium incorporation into Csk in the presence of ADP. These studies are directed at localizing any structural effects induced by substrate phosphorylation to specific regions in the polypeptide chain, a pursuit that could offer insights into the nature of the slow, rate-limiting structure changes in Csk. Figure 5(b) displays the protected probes for Csk in the presence of ADP. While many of the probes protected by AMPPNP are equally protected by ADP (light blue regions), several key

probes observe noticeable differences. In the kinase domain, the glycine-rich loop is more protected by ADP than AMPPNP (L200-M21 in Figure 4; dark blue in Figure 5(b)). This could result partly from structural changes in the loop after phosphoryl transfer to the substrate. While it is difficult to know the molecular nature of this change, it is conceivable that the loop more adequately covers the diphosphate moiety of ADP compared to the triphosphate in ATP. Such motions may be necessary for configuring the γ phosphate group into a productive form.

In addition to local effects on the glycine-rich loop, ADP has profound effects on the activation loop. In this region, ADP protects the loop to a lower extent than AMPPNP (G334-L358; Figures 4 and 5(b)), suggesting that this region of the kinase domain may exhibit higher flexibility or solvent exposure after the delivery of the γ phosphate group. This effect is not localized to the activation loop but rather is coupled to other motions within the large lobe. For example, helix αG is less protected in the presence of ADP than AMPPNP, a phenomenon that may reflect synchronous motions in this location (G383-G402, Figures 4 and 5(b)). Whatever the cause, it is clear that delivery of the phosphoryl donor has pervasive effects on the kinase domain. These motions are also coupled to changes in two interfacial probes. The probes corresponding to helix αA in the SH2 domain and the SH2-kinase linker are more flexible in the presence of ADP than AMPPNP (Figure 5(b)). Again, as we have seen with our study of AMPPNP binding, ADP has long-range effects on the solution conformation of Csk. The nature of these long-range effects are markedly different depending on the presence of the γ phosphate group in the nucleotide pocket. Such a striking contrast between hydrogen exchange properties as a function of substrate (AMPPNP) and product (ADP) may result from distinct conformational states. Since conformational dynamics limit substrate processing in this enzyme (Figure 1), the definition of critically affected regions will be useful for the understanding of protein phosphorylation.

Materials and Methods

Materials

Guanidine hydrochloride was purchased from Gibco BLR and was of ultra pure quality. ADP, 5′-adenylyl-imidodiphosphate (AMP-PNP), thrombin, glutathione immobilized on 4% (w/v) beaded agrose, glutathione, and Mops were obtained from Sigma. Formic acid was obtained from Fisher. $^{2}H_2O$ (99% deuterium) was purchased from ISOTEC Inc. H-^{2}H-Phe-Pro-Arg-chloromethylketone trifluoroacetate salt (p-PACK) was obtained from Bachem.

Protein preparation and activity assay

Human Csk was expressed in *Escherichia coli* as a GST-Csk fusion protein and purified as described.[19] The fusion protein was cleaved with thrombin at 25 °C for 90 minutes. The mixture was subjected to treatment with p-PACK for 30 minutes to inactivate thrombin. Csk was separated from GST and uncleaved fusion protein using a Q Sepharose column (Pharmacia) with a 50 mM–300 mM NaCl gradient. The protein was dialyzed into a buffer containing 25 mM potassium phosphate (pH 7.6), and concentrated to 109 μM. The protein was stored at −80 °C in small aliquots and used in experiments without glycerol. The activity of Csk was measured using a spectrophotometric coupled enzymatic assay (Shaffer & Adams) and was comparable to published data.[19]

DXMS apparatus

Equipment configuration for these studies consisted of high-pressure switching valves (Rheodyne 7010) connected to pumps and other components with PEEK tubing (Upchurch Scientific); a Spectraphysics AS3000 autosampler (Thermo Finnigan LLC, San Jose, CA) in which all but 20 of the sample vial positions were filled with powdered dry ice; a pepsin-20AL column (66 μl bed volume, porcine pepsin (Sigma) coupled to 20AL support material per the manufacturer's instructions (PerSeptive Biosystems); a C18 column (1 mm × 50 mm, Vydac cat. No. 218MS5105). Four HPLC pumps (Shimadzu LC-10AD, operated by a Shimadzu SCL-10A pump controller); one pump delivered 0.05% aqueous TFA to push samples through the pepsin column; and another delivered the same buffer to backflush the pepsin column after sample digestion. Two additional pumps delivered solvents for HPLC column gradient elution (pump A 0.05% aqueous TFA and pump B 80% acetonitrile, 20% water, 0.01% TFA). Inline filters (0.5 μm, Upchurch cat. No. A.430) were placed on each side of the pepsin column and just before the C18 column (Vydac prefilter, cat. No. CPF 10) to minimize column fouling and carryover of aggregated material. To provide precise temperature control, valves, tubing, columns and autosampler were contained within a refrigerator maintained at 2.8 °C, with columns also immersed in melting ice. Mass spectrometric analyses were carried out with a Finnigan LCQ electrospray ion trap type mass spectrometer (Thermo Finnigan) with capillary temperature at 200 °C.

General operational procedure

Sets of autosampler vials containing quenched, functionally deuterated samples (50 μl, stored at −80 °C) were placed in the dry ice-containing sample basin of the autosampler. The samples were held there at dry ice temperature until individually melted by the autosampler at 2–3 °C over 1.5 minutes, utilizing its sample preparation features, and then injected (45 μl) onto the pepsin column. The samples were pumped through the pepsin column (0.05% TFA at 100 μl/minute) with contemporaneous collection of digestion products on the C18 HPLC column. The digested peptides were separated by a linear acetonitrile gradient (5 → 45% B/ten minutes; 50 μl/minute; solvent A, 0.05% TFA; solvent B, 80% acetonitrile, 20% water, 0.01% TFA). The mass spectrometer acquired spectra on the effluent in either MS1 profile mode, or data-dependent MS2 mode.

Optimization of fragmentation conditions

Two major parameters optimized were the concentration of GuHCl in the quenching buffer and the sample flow rate over the pepsin column. A 2 μl stock solution of CSK (5.8 mg/ml) was diluted with 18 μl of water, then quenched with 30 μl of 0.8% formic acid containing various concentrations of GuHCl (0–6.4 M), and then frozen in autosampler vials on dry ice. The quenched, frozen samples were later processed in the DXMS apparatus (above) employing a range of flow rates over the pepsin column (100–300 μl/minute).

Sequence identification of pepsin-generated peptides

To quickly identify pepsin-generated peptides for each digestion condition employed, spectral data were acquired in "triple play" mode. The triple play data set was then analyzed employing the Sequest software program (Thermo Finnigan Inc) to identify the sequence of the dynamically selected parent peptide ions. This tentative peptide identification was verified by visual confirmation of the parent ion charge state presumed by the Sequest program for each peptide. This set of peptides was then further examined to determine if the "quality" of the measured isotopic envelope of peptides was sufficient to allow accurate measurement of the geometric centroid of isotopic envelopes on deuterated samples.

Deuterium exchange experiments

All exchange mixtures for Csk contained the following: 9.8 nM Csk, 18 mM Mops, 45 mM NaCl, 0.9 mM DTT. Final pH was 7.0, and final percentage of ^2H_2O was 90%. Exchange experiments in the presence of nucleotides included 1 mM ADP and 2 mM AMP-PNP with 11 mM $MgCl_2$ and 12 mM $MgCl_2$, respectively. Csk was pre-equilibrated with the respective nucleotides in H_2O before starting the deuterium exchange by diluting into ^2H_2O. The ^2H_2O mixture was prepared as follows. Appropriate amounts of Mops, NaCl, and DTT were dissolved in ^2H_2O and mixed with deuterated solutions of nucleotide and $MgCl_2$. The final mixture contained 20 mM Mops, 50 mM NaCl, 1 mM DTT, and either 1 mM ADP and 11 mM $MgCl_2$, or 2 mM AMP-PNP and 12 mM $MgCl_2$. The H_2O mixtures contained 98 nM Csk, and either 1 mM ADP and 11 mM $MgCl_2$, or 2 mM AMP-PNP and 12 mM $MgCl_2$. Deuterium exchange was initiated by the addition of 20 μl of the H_2O solutions to 180 μl of the ^2H_2O solutions. The solutions were incubated on ice. At various times, 20 μl aliquots were removed and added to an ice-cold tube containing 30 μl of 0.8% formic acid with 0.8 M GuHCl. This brought the Csk solution down to pH 2.5 and quenched the deuterium exchange. The quenched samples were frozen in dry ice and stored at −80 °C prior to ESI MS analysis. Freeze-thawing did not significantly affect the extent of deuterium incorporation (data not shown).

In and back-exchange controls

Controls were performed as described.[26] Briefly, in-exchange of deuterium under quench conditions was measured by adding the protein solution directly to a mix of the ^2H_2O solution and quench solution and performing the remaining procedure as normal. This sample corresponds to time-point zero. The back-exchange was determined by incubating Csk in ^2H_2O containing 0.5% formic acid overnight at 25 °C. This allows for complete exchange of backbone amide protons for deuterium. To determine the amount of label lost during the experiment (i.e. back-exchange) the deuterated sample was treated with quench solution and subjected to ESI MS analysis as described above. This control provides, for each peptide, the maximal experimental mass that relates to a fully exchanged peptide. To confirm that the conditions employed were sufficient to fully (equilibrium) deuterate the intact protein, Csk was first proteolyzed on the pepsin column, as above, effluent peptides collected in bulk, dried, and peptides taken up and incubated in ^2H_2O containing 0.5% formic acid overnight at 25 °C, subesquent LCMS analysis of these deuterated peptides was performed as for the intact Csk except that the pepsin column was bypassed to avoid re-digestion. The deuterium content of corresponding peptides was identical with the two methods of deuteration (data not shown).

Calculation of deuteration level

The centroids of probe peptide isotopic envelopes were measured using the method of Zhang & Smith employing the Magtran program[31] as well as employing specialized software that fully automates the centroiding procedure (Sierra Analytics, LLC, Modesto, CA). Corrections for back-exchange were made employing the methods of Zhang & Smith:[31]

$$\text{Deuterium incorporation}(\#) = \frac{m(\text{P}) - m(\text{N})}{m(\text{F}) - m(\text{N})}\text{MaxD} \qquad (1)$$

where m(P), m(N), and m(F) are the centroid value of partially deuterated peptide, non-deuterated peptide, and fully deuterated peptide, respectively. MaxD is the maximum deuterium incorporation calculated by subtracting the number of proline residues in the third or later amino acid and two from the number of amino acid residues in the peptide of interest (assuming the first two amino acid residues cannot retain deuterons. The average deuteron recovery of fully deuterated sample [(m(F) − m(N))/MaxD] was 79%.

Acknowledgements

We thank Walter Englander, David Smith, David Wemmer, and Dennis Pantazatos for their considerable help and guidance in the development and implementation of DXMS. We also thank the W. M. Keck Foundation for the use of their computer facility. These studies were funded by University of California BioStar Technology transfer grants S97-90 and S99-44 (V.L.W.); University of California Life Sciences Informatics (LSI) Technology transfer grant L98-30 (V.L.W.), NIH (DK5441) to P.A.J., NIH/NCI NRSA (T32 CA09523) to L.W. and by NIH (CA 75112) and NSF grants (0111068) to J.A.A. ExSAR Corporation, Inc. is the matching partner for the technology transfer grants. V.L.W. & Y.H. have financial interests in ExSAR Corporation, Inc.

References

1. Superti-Furga, G. & Courtneidge, S. A. (1995). Structure–function relationships in Src family and related protein tyrosine kinases. *BioEssays*, **17**, 321–330.
2. Neet, K. & Hunter, T. (1996). Vertebrate non-receptor protein-tyrosine kinase families. *Genes Cells*, **1**, 147–169.
3. Tatosyan, A. G. & Mizenina, O. A. (2000). Kinases of the Src family: structure and functions. *Biochemistry (Mosc)*, **65**, 49–58.
4. Okada, M., Nada, S., Yamanashi, Y., Yamamoto, T. & Nakagawa, H. (1991). CSK: a protein-tyrosine kinase involved in regulation of src family kinases. *J. Biol. Chem.* **266**, 24249–24252.
5. Bergman, M., Mustelin, T., Oetken, C., Partanen, J., Flint, N. A., Amrein, K. E. *et al.* (1992). The human p50csk tyrosine kinase phosphorylates p56lck at Tyr505 and down regulates its catalytic activity. *EMBO J.* **11**, 2919–2924.
6. Inomata, M., Takayama, Y., Kiyama, H., Nada, S., Okada, M. & Nakagawa, H. (1994). Regulation of Src family kinases in the developing rat brain: correlation with their regulator kinase, Csk. *J. Biochem. (Tokyo)*, **116**, 386–392.
7. Latour, S. & Veillette, A. (2001). Proximal protein tyrosine kinases in immunoreceptor signaling. *Curr. Opin. Immunol.* **13**, 299–306.
8. Taylor, S. J. & Shalloway, D. (1996). Src and the control of cell division. *BioEssays*, **18**, 9–11.
9. Zenner, G., Dirk zur Hausen, J., Burn, P. & Mustelin, T. (1995). Towards unraveling the complexity of T cell signal transduction. *BioEssays*, **17**, 967–975.
10. Hamaguchi, I., Yamaguchi, N., Suda, J., Iwama, A., Hirao, A., Hashiyama, M. *et al.* (1996). Analysis of CSK homologous kinase (CHK/HYL) in hematopoiesis by utilizing gene knockout mice. *Biochem. Biophys. Res. Commun.* **224**, 172–179.
11. Lamers, M. B., Antson, A. A., Hubbard, R. E., Scott, R. K. & Williams, D. H. (1999). Structure of the protein tyrosine kinase domain of C-terminal Src kinase (CSK) in complex with staurosporine. *J. Mol. Biol.* **285**, 713–725.
12. Sicheri, F., Moarefi, I. & Kuriyan, J. (1997). Crystal structure of the Src family tyrosine kinase Hck. *Nature*, **385**, 602–609.
13. Williams, J. C., Weijland, A., Gonfloni, S., Thompson, A., Courtneidge, S. A., Superti-Furga, G. & Wierenga, R. K. (1997). The 2.35 Å crystal structure of the inactivated form of chicken Src: a dynamic molecule with multiple regulatory interactions. *J. Mol. Biol.* **274**, 757–775.
14. Xu, W., Harrison, S. C. & Eck, M. J. (1997). Three-dimensional structure of the tyrosine kinase c-Src. *Nature*, **385**, 595–602.
15. Ogawa, A., Takayama, Y., Sakai, H., Chong, K. T., Takeuchi, S., Nakagawa, A. *et al.* (2002). Structure of the carboxyl-terminal Src kinase, Csk. *J. Biol. Chem.* **277**, 14351–14354.
16. Grant, B. D. & Adams, J. A. (1996). Pre-steady-state kinetic analysis of cAMP-dependent protein kinase using rapid quench flow techniques. *Biochemistry*, **35**, 2022–2029.
17. Shaffer, J. & Adams, J. A. (1999). Detection of conformational changes along the kinetic pathway of protein kinase A using a catalytic trapping technique. *Biochemistry*, **38**, 12072–12079.
18. Shaffer, J. & Adams, J. A. (1999). An ATP-linked structural change in protein kinase A precedes phosphoryl transfer under physiological magnesium concentrations. *Biochemistry*, **38**, 5572–5581.
19. Shaffer, J., Sun, G. & Adams, J. A. (2001). Nucleotide release and associated conformational changes regulate function in the COOH-terminal src kinase, csk. *Biochemistry*, **40**, 11149–11155.
20. Jan, A. Y., Johnson, E. F., Diamonti, A. J., Carraway, I. K. & Anderson, K. S. (2000). Insights into the HER-2 receptor tyrosine kinase mechanism and substrate specificity using a transient kinetic analysis. *Biochemistry*, **39**, 9786–9803.
21. Sivaraman, T., Arrington, C. B. & Robertson, A. D. (2001). Kinetics of unfolding and folding from amide hydrogen exchange in native ubiquitin. *Nature Struct. Biol.* **8**, 331–333.
22. Rodriguez, H. M., Robertson, A. D. & Gregoret, L. M. (2002). Native state EX2 and EX1 hydrogen exchange of *Escherichia coli* CspA, a small beta-sheet protein. *Biochemistry*, **41**, 2140–2148.
23. Chamberlain, A. K. & Marqusee, S. (1997). Touring the landscapes: partially folded proteins examined by hydrogen exchange. *Structure*, **5**, 859–863.
24. Englander, S. W., Mayne, L., Bai, Y. & Sosnick, T. R. (1997). Hydrogen exchange: the modern legacy of Linderstrom-Lang. *Protein Sci.* **6**, 1101–1109.
25. Engen, J. R. & Smith, D. L. (2001). Investigating protein structure and dynamics by hydrogen exchange MS. *Anal. Chem.* **73**, 256A–265A.
26. Andersen, M. D., Shaffer, J., Jennings, P. A. & Adams, J. A. (2001). Structural characterization of protein kinase A as a function of nucleotide binding: hydrogen–deuterium exchange studies using MALDI-TOF MS detection. *J. Biol. Chem.* **276**, 14204–14211.
27. Jeffrey, P. D., Russo, A. A., Polyak, K., Gibbs, E., Hurwitz, J., Massague, J. & Pavletich, N. P. (1995). Mechanism of CDK activation revealed by the structure of a cyclinA-CDK2 complex. *Nature*, **376**, 313–320.
28. Hubbard, S. R. (1997). Crystal structure of the activated insulin receptor tyrosine kinase in complex with peptide substrate and ATP analog. *EMBO J.* **16**, 5572–5581.
29. Englander, S. W. & Kallenbach, N. R. (1983). Hydrogen exchange and structural dynamics of proteins and nucleic acids. *Quart. Rev. Biophys.* **16**, 521–655.
30. Thevenon-Emeric, G., Kozlowski, J., Zhang, Z. & Smith, D. L. (1992). Determination of amide hydrogen exchange rates in peptides by mass spectrometry. *Anal. Chem.* **64**, 2456–2458.
31. Zhang, Z. & Smith, D. L. (1993). Determination of amide hydrogen exchange by mass spectrometry: a new tool for protein structure elucidation. *Protein Sci.* **2**, 522–531.
32. Woods, V. L., Jr & Hamuro, Y. (2001). High resolution, high-throughput amide deuterium exchange-mass spectrometry (DXMS) determination of protein binding site structure and dynamics: utility in pharmaceutical design. *J. Cell. Biochem.* **Suppl**, 89–98.
33. Woods, V. L., Jr (1997). Method for characterization of the fine structure of protein binding sites. US Patent #5,658,739, The Regents of the University of California, USA.
34. Woods, V., Jr (2001). Methods for the high-resolution identification of solvent-accessible amide hydrogens in polypeptides or proteins and for the characterization of the fine structure of protein binding sites. US Patent #6,291,189, Carta Proteomics, Inc., USA.

35. Woods, V., Jr (2001). Method for characterization of the fine structure of protein binding sites. US Patent #6,331,400, Carta Proteomics, Inc., USA.
36. Resing, K. A. & Ahn, N. G. (1997). Protein phosphorylation analysis by electrospray ionization-mass spectrometry. *Methods Enzymol.* **283**, 29–44.
37. Resing, K. A. & Ahn, N. G. (1998). Deuterium exchange mass spectrometry as a probe of protein kinase activation. Analysis of wild-type and constitutively active mutants of MAP kinase kinase-1. *Biochemistry*, **37**, 463–475.
38. Resing, K. A., Hoofnagle, A. N. & Ahn, N. G. (1999). Modeling deuterium exchange behavior of ERK2 using pepsin mapping to probe secondary structure. *J. Am. Soc. Mass Spectrom.* **10**, 685–702.
39. Knighton, D. R., Zheng, J. H., Ten Eyck, L. F., Xuong, N. H., Taylor, S. S. & Sowadski, J. M. (1991). Structure of a peptide inhibitor bound to the catalytic subunit of cyclic adenosine monophosphate-dependent protein kinase. *Science*, **253**, 414–420.
40. Knighton, D. R., Zheng, J. H., Ten Eyck, L. F., Ashford, V. A., Xuong, N. H., Taylor, S. S. & Sowadski, J. M. (1991). Crystal structure of the catalytic subunit of cyclic adenosine monophosphate-dependent protein kinase. *Science*, **253**, 407–414.
41. Johnson, L. N., Noble, M. E. & Owen, D. J. (1996). Active and inactive protein kinases: structural basis for regulation. *Cell*, **85**, 149–158.
42. Hubbard, S. R., Wei, L., Ellis, L. & Hendrickson, W. A. (1994). Crystal structure of the tyrosine kinase domain of the human insulin receptor (see comments). *Nature*, **372**, 746–754.
43. Sondhi, D. & Cole, P. A. (1999). Domain interactions in protein tyrosine kinase Csk. *Biochemistry*, **38**, 11147–11155.
44. Sun, G. & Budde, R. J. (1999). Mutations in the N-terminal regulatory region reduce the catalytic activity of Csk, but do not affect its recognition of Src. *Arch. Biochem. Biophys.* **367**, 167–172.

Edited by P. Wright

(Received 12 March 2002; received in revised form 11 September 2002; accepted 12 September 2002)